JOURNAL OF WATER AND LAND DEVELOPMENT

Drought prediction in the Lepelle River basin, South Africa under general circulation model simulations

Darlington C. IKEGWUOHA[1] ✉, Megersa O. DINKA[2]

[1] University of Johannesburg, Department of Civil Engineering Science, PO Box 524, Auckland Park, Johannesburg, Gauteng, 2006, South Africa; Durban University of Technology, Durban, South Africa

[2] University of Johannesburg, Department of Civil Engineering Science, Johannesburg, Gauteng, South Africa

Abstract

This study aims to evaluate changes in the frequency and severity of historical droughts (1980–2018) and then model future droughts occurrences (2019–2099) in the Lepelle River Basin (LRB), using Intergovernmental Panel on Climate Change (IPPC) General Circulation Model (GCM) simulations for two representative concentration pathways (RCP8.5 and RCP4.5). Firstly, the present-day and future hydrology of the LRB are modelled using the weather evaluation and planning (WEAP) model. Mann–Kendall tests are conducted to identify climate trends in the LRB. The reconnaissance drought index (*RDI*) and the streamflow drought index (*SDI*) are employed to explore hydro-meteorological droughts in the Lepelle River Basin, South Africa. The *RDI* and *SDI* are plotted over time to assess drought magnitude and duration. The simulated temporal evolution of *RDI* and *SDI* show a significant decrease in wetting periods and a concomitant increasing trend in the dry periods for both the lower and middle sections of the LRB under RCP4.5 as the 22nd century is approached. Lastly, the Spearman and Pearson correlation matrix is used to determine the degrees of association between the *RDI* and *SDI* drought indices. A strong positive correlation of 0.836 is computed for the middle and lower sections of the LRB under the RCP8.5 forcing. Further findings indicate that severe to extreme drought above –2.0 magnitude are expected to hit the all three sections of the LRB between 2080 and 2090 under RCP8.5. In the short term, it is suggested that policy actions for drought be implemented to mitigate possible impacts on human and hydro-ecological systems in the LRB.

Key words: *drought, high-resolution-climate-data, Lepelle-River-Basin, representative concentration pathways (RCPs), weather evaluation and planning (WEAP)*

INTRODUCTION

It has been established worldwide that climate variability exists on all time scales, and floods and droughts are extremes associated with variability in precipitation [ZHU *et al.* 2017]. Adding to climate variability, climate change has been identified as a key driver for modifying the hydrological cycle via global warming. Climate change refers to any long-term (over at least 30 years), significant change in the expected patterns of average weather in a specific region [WATKINS 2007]. Climate change in the negative direction can lead to a total annihilation and disappearance of cities. A good example is the disappearance of the Mayan cities of South America [TURNER, SABLOFF 2012]. Analogously, it has been widely acknowledged that the frequency and magnitude of extreme hydrologic events can be modulated by enhanced climate variability due to climate change. Relatedly, according to the precipitation outlook based on climate change scenarios , increasing concentrations of greenhouse gases are likely to result in very different patterns of heavy rain, extreme drought, and heavy snow in some regions [YOO *et al.* 2012]. There is a collective agreement that in recent decades, extreme drought events seem to be growing in frequency in many countries [SPINONI *et al.* 2014], including South Africa. For example, between 2017 and 2018, South Africa expe-

rienced one of the worst droughts in history. One of the cities that was hardest hit was Cape Town where several measures were put in place to avoid "Day Zero" (dam levels below 13.5%) [PARKS *et al.* 2019]. Similarly, in KwaZulu-Natal seldom tornadoes date back to the 1900s but within 24 hours two tornadoes accompanied by above average monthly rainfall devasted the cities of KwaZulu-Natal these occurred on 22 and 23 November 2019 according to "Daily News KwaZulu natal" [KUBHEKA 2019]. These extreme events point directly to the impacts of runaway climate change.

MATERIALS AND METHODS

STUDY AREA

The Lepelle River Basin (LRB), formerly known as the Olifants River Basin, is one of Southern Africa's most important catchments. Geographically, the Lepelle River Basin is in the northeastern corner of South Africa and southern Mozambique bounded by coordinates 23°46'24.0" S to 26°33'40" S and 28°19'28.5" E to 31°57'25.5" E (Fig. 1). The Lepelle River is approximately 770 km long and, with its tributaries, drains 54,570 km^2 which is an area equivalent to the size of Slovakia or Croatia. Its waters irrigate farming across the western section of the Mpumalanga Province in South Africa and supply water to several coal operated power stations in the area. The river flows also through the Limpopo Province's platinum belt and supplies water to several mines. It then flows through the Drakensberg mountains and down the escarpment to irrigate farms in the "Lowveld" (situated in Mpumalanga Province of South Africa) and brings life to the Kruger National Park. It finally joins the Limpopo River in Mozambique, before flowing into the Indian Ocean South of Xai-Xai. This makes the river critical to the economies
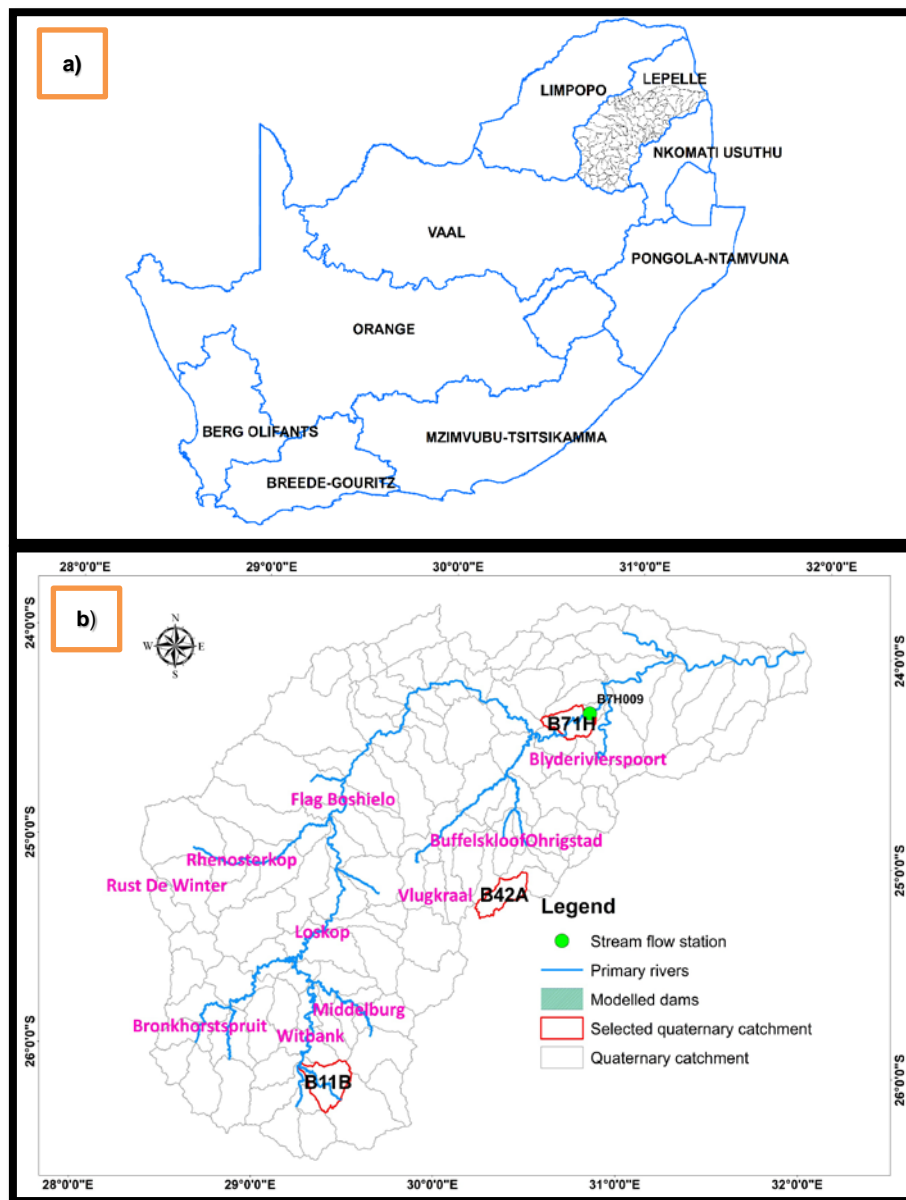

Fig. 1. Location map: a) the nine Water Management Areas of South Africa, b) the Lepelle River Basin with the Quaternary catchments, the Lepelle River and its major tributaries, streamflow stations and dams; source: own elaboration

of both South Africa and Mozambique [POLLARD *et al.* 2018]. The 30 dams along its course also provide water to three provinces during times of drought and approximately ten million people rely on this water.

In terms of water security, according to the Association for Water and Rural Development report [POLLARD *et al.* 2018], the Lepelle River, it was noted that in 2005 the river stopped flowing for 78 days despite the fact that it was not in a "dry cycle" a similar stoppage occurred in January 2016 and January 2018, prompting widespread concern and calls for an integrated focus on all the easterly-flowing rivers of the Lowveld of South Africa. The Lepelle River Basin is a significant basin because it is the largest contributor of flows to the transboundary Limpopo River. Despite the enabling legislative framework for water reform in South Africa introduced in 1998, most rivers in this catchment continue to degrade in both quality and quantity. Given that these rivers form part of transboundary hydrological systems, the implications are of wider geographical significance across sub-Saharan Africa. Indeed, flows into Mozambique support the livelihoods of between 6,000 and 10,000 small-scale farmers and mangroves which are a critical conservation priority [POLLARD *et al.* 2018]. Thus, changes in flow and water quality will have major impacts and highlight the importance of a systemic approach to drought resilience in the region.

Three representative Quaternary catchments of the 114 Quaternary catchments namely B11B, B42A and B71H were selected for discussion in this study. B11B is in the upper LRB, B42A is almost centrally located and falls into the middle LRB while B71H falls in the lower LRB with elevations of 1578 m, 1597 m and 504 m respectively and mean annual precipitations of 701.2 mm, 640.2 mm and 668.3 mm respectively. Figure 1 also shows the streamflow gauge used for calibrating the model was located at catchment B71H.

Between 2016 and 2018, the lower part of the LRB saw one of the most severe droughts in history. Prior to this the LRB also experienced other extreme events, such as the floods in 2000 and 2012. Various studies [CONDIE, LEE 1982; DALRYMPLE 1960; MAGHSOOD *et al.* 2019; ORSINI-ZEGADA, ESCALANTE-SANDOVAL 2016] have investigated aspects related to these flood events but little has been done in terms of drought prediction. There is evidence for the spatiotemporal variation of droughts, which take the form of band-limited and quasi-oscillatory variations, linked with the El Niño–Southern Oscillation (ENSO). This paper seeks to interrogate and identify future hydro-meteorological droughts using two drought indices: namely the reconnaissance drought index (*RDI*) and the streamflow drought index (SDI). Some studies have attempted to analyse drought intensity and duration using wavelet analysis [GYAMFI *et al.* 2019] while others have tried to analyse drought frequency using Global Wavelet Power [LEE *et al.* 2016]. GONZÁLEZ, VALDÉS [2010] advocated for the use of mean frequency of occurrence (MFR) to analyse and characterise drought. Although, the frequency of a specific hydrologic variable should not be treated independently of the frequency of the generating mechanisms. [LEE *et al.* 2012] Hence there is a need to predict drought occurrences via warning signals with sufficient lead time to implement mitigation strategies. To achieve this, the present-day and future hydrology of the LRB is determined under two scenarios of climate change using the weather evaluation and planning (WEAP) model. It is used to simulate future streamflow of the LRB as well as explore and fit probability distribution functions (PDFs) to the future hydro-meteorological variables in order to identify meteorological and hydrological droughts at different time scales using the two different indices (*RDI* and *SDI*). Finally, trend analysis is carried out on future streamflow and rainfall variables using Mann–Kendall trend analysis to determine if a discernible trend in the patterns of drought exist.

DATA

Scientific uncertainties

Three major sources of uncertainties that have not been overcome in climate modelling studies are as follows. First is the uncertainty associated with the selection of a climate change scenario. This uncertainty relates to projections of future greenhouse gas concentrations [MAURER 2007]. The second uncertainty is the limited ability of GCMs to reproduce a future climate based on the selected emission scenario. The third uncertainty results from biases in the statistical downscaling approach. This study employed six GCMs (ACCESS, CCSM, CNRM, GDFL, MPI-ESM and Nor-ESM1-M) to characterize the uncertainties when investigating the variability of drought under scenarios of climate change (see Tab. 1).

Simulated climate variables from the GCMs are examined for similar statistical characteristics using three approaches. The first approach compares the statistical properties of the simulated data with that of the observed from the LRB weather station during the historical period (intra and inter annual variability and timing). Then statistical hypothesis tests (i.e., *t*-test and *F*-test) are used to determine if the mean and variance of the observed and simu-

Table 1. Global Circulation Models used as source data for downscaling

Acronym	Meaning	Location	Reference
ACCESS	Australian Community Climate and Earth System Simulator	Australia	PURI [2005]
CCSM	NCAR/UCAR Community Climate System Model	USA	COLLINS *et al.* [2006]
CNRM	Centre National de Recherches Météorologiques	France	BORDERIES *et al.* [2019]
GFDL	Geophysical Fluid Dynamics Laboratory	Princeton University USA formerly known as college of New Jersey	LIN *et al.* [1994]
MPI-ESM	Max Planck Institute Earth System Mode	Germany	GIORGETTA *et al.* [2013]
NorESM1-M	Norwegian Earth System Model	Norway	BENTSEN *et al.* [2013]

Source: own elaboration based on the references in column 4.

Table 2. Descriptive statistics for observed and simulated streamflow (m^3)

Value	Mean	Median	Mode	Min	*SD*	*CV*
Streamflow statistics						
Simulated	$9.91 \cdot 10^7$	$5.00 \cdot 10^7$	$1.19 \cdot 10^9$	$3.38 \cdot 10^6$	$1.51 \cdot 10^8$	152.06
Observed	$1.31 \cdot 10^8$	$4.32 \cdot 10^7$	$1.46 \cdot 10^9$	$7.72 \cdot 10^5$	$2.29 \cdot 10^8$	175.12
Percentage difference (%)						
Absolute	24.14	15.79	18.99	338.13	34.13	13.16

Explanations: *SD* = standard deviation, *CV* = coefficient of variation.
Source: own elaboration based on model results from the modelled LRB hydrology.

lated data are significantly different from each other, respectively [SEMENOV, BARROW 1997]. The second approach compares various statistical variables, namely the mean, median and maximum values of the simulated climate variables with historical data. The third approach simulates streamflow of the LRB using WEAP and then compares it with observed streamflow at a streamflow gauge (B7H009). The reason for using only one gauge is because this station provided the most comprehensive dataset. The 8 km resolution data from the Centre for Scientific and Industrial Research (CSIR) was established to be very similar to the historical data by comparing their means, standard deviations, coefficient of variations and maximums as seen in Table 2 it was then used for the WEAP model.

The descriptive statistics presented in Table 2 indicate that the observed and simulated data are positively correlated. Also, the Student *t*-test is equal to zero at a 0.05 significance level. Coefficient of determination is 0.7169 for the calibration period and 0.706 for the validation period and the slope is close to 1 and intercept close to 0 as suggested [AHNERT *et al.* 2007]. Other data that were incorporated into the model include, crop coefficient for the major crops grown in the regions, latitude, runoff resistance factor, preferred flow direction, demand sites, withdrawal nodes, reservoirs and their various operating systems and various other requirements of the model. Data for each demand sites included water demand arising from industrial, energy, agricultural, mining, urban and rural water demands. These data were projected to 2035 and, in some cases, to 2040 by the report. However, projections for these demands up to 2099 were extrapolated using two major growth scenarios (high growth and low growth). Downscaling methods that reproduce a future climate based on selected emission scenarios are used to overcome the uncertainty related to the limited ability of GCMs.

Downscaling of GCMS

GCMs are a powerful tool to perform climate projections at a global scale, but they are generally unsuitable to provide climate data for impact studies as they are characterised by coarse resolutions of 1–5 degrees in latitude or longitude. This resolution is not suitable to analyse some important phenomena that occur at spatial scales of tens of kilometres. In addition, local topographic peculiarities such as rain shadows or wind tunnel effects are often not identified by global models with resolutions of 250×250 km per grid cell. Thus, in order to analyse local and regional scales, the global climate models must be downscaled to

resolutions between 1×1 km and 50×50 km [ENGELBRECHT *et al.* 2011; SMID, COSTA 2018].

Two downscaling techniques can be distinguished: dynamical downscaling e.g. THATCHER *et al.* [2015], using high-resolution, numerical regional climate models, and statistical downscaling e.g. SCHMIDLI *et al.* [2007], based on statistical relationships between large-scale predictor variables and regional ones. Each technique has advantages and disadvantages. Dynamical downscaling simulates climate mechanisms without any previous assumptions about relationships between the current and the future climate. This is because history is not a good predictor of the future. Rainfall and other climate variables such as temperature, wind speed and relative humidity have significant variability, are distinctively non-Gaussian, exhibit relatively complicated spatiotemporal dependence and cannot be easily derived from atmospheric dynamic equations. Although advanced, dynamical downscaling comes with the constraints of being expensive in terms of computing resources and professional expertise. It may also be sensitive to uncertain parameterizations and may propagate biases from the GCM to the regional scale. Statistical downscaling is much cheaper to perform from a computational perspective and may correct for biases of the GCM. However, it assumes that the relationships between large-scale and local climate are constant (stationarity). It also requires substantial amounts of observed data and does not capture climate mechanisms.

One of the most effective tools for providing high-resolution climate analysis through downscaling is represented by regional climate models (RCMs), which can provide an accurate description of climate variability at a regional scale. Moreover, RCMs show the capacity to provide a detailed description of climate extremes that are often more important than mean values which is critical for the research presented here. In order to capture explicit effects, downscaling techniques are applied to the global circulation models, resulting in projections with resolutions of 50×50 km to 8×8 km per grid cell or finer. As the grid cells become smaller, the computational costs (in terms of elapsed time) become higher, which is why very few high-resolution experiments with grid cells of 1×1 km are currently conducted for small areas [ENGELBRECHT *et al.* 2011]. These researches applied both techniques within the CLUVA project and a multimodal ensemble of simulations of present-day and future climate has been made available for each of the South African cities spanning 1961–2099.

The data provided by ENGELBRECHT *et al.* [2011] include precipitation, temperature, wind speed and relative humidity. These data were useful for modelling the future

hydrology of the LRB under climate change projections using two emission scenarios, namely the RCP8.5 and RCP4.5 scenarios.

Representative concentration pathway (RCP) 4.5. RCP4.5 is a scenario of long-term, global emissions of greenhouse gases, short-lived species, and land-use-land-cover which stabilizes radiative forcing at 4.5 W·m^{-2} (approximately 650 ppm CO_2-equivalent) in the year 2100 without ever exceeding that value [THOMSON *et al.* 2011]. Population and economic growth are moderate. Oil consumption is estimated to remain fairly constant through to 2100. Nuclear power and renewables play an increasingly greater role. Significantly, cropping and grassland area declines while reforestation increases the area of natural vegetation [WAYNE 2013]. It was generated by the global change assessment model (GCAM) [WISE *et al.* 2009].

Representative concentration pathway (RCP) 8.5. RCP8.5 is the last scenario in the AR5 report. It represents the nightmare scenario in which emissions continue to increase rapidly through the early and mid-parts of the 21st century. By 2100 annual emissions have stabilised at just under 30 Gt of carbon compared to around 8 Gt in 2000 [WAYNE 2013]. Rising radiative forcing pathway which leads to 8.5 W·m^{-2} (~1370 ppm CO_2) by 2100 [RIAHI *et al.* 2011]. Concentrations of CO_2 in the atmosphere increase to 950 ppm by 2100 and continue increasing for an additional 100 years. Population growth is high, reaching 12 billion by the end of the 21st century. This scenario is highly energy intensive with total consumption continuing to grow throughout the century reaching well over three-times current levels. Oil use grows rapidly until 2070 after which it drops even more quickly. Coal provides the bulk of the large increase in energy consumption. Land use continues current trends with crop and grass areas increasing and forest area decreasing [RIAHI *et al.* 2011]. It was developed by the model for energy supply strategy alternatives and their general environmental impact (MESSAGE).

The six GCMs were averaged and then used for modelling the present-day and future hydrology of the LRB under climate change with emphasis on future drought predictions. The Quaternary catchments (QCs) were chosen for analysis each from one of the broader LRB catchments (Upper Lepelle-B11B, Middle Oliants-42A and Lower Lepelle-71H). Below are the methods used to evaluate the future drought situation for the LRB.

Streamflow data

Historical streamflow data used in this research was obtained from the National Department of Water and Sanitation (DWS). The future streamflow data was generated from the LRB future hydrology model. The LRB future and present-day hydrology was modelled using weather evaluation and planning (WEAP). WEAP's soil moisture-method was used to model the LRB hydrology. WEAP operates on the basic principle of water balance accounting, WEAP is applicable to municipal and agricultural systems, single sub-basins or complex river systems. Moreover, WEAP can address a wide range of issues, including sectoral demand analyses, water conservation, water rights

and allocation priorities, groundwater and streamflow simulations, reservoir operations, hydropower generation and energy demands, pollution tracking, ecosystem requirements, and project benefit-cost analyses.

The analyst represents the system in terms of its various supply sources (e.g., rivers, streams, groundwater, reservoirs), withdrawal, transmission, and wastewater treatment facilities; ecosystem requirements, water demands and pollution generation. The data structure and level of detail can be customized to meet the requirements of a particular analysis, and to reflect the limits imposed by restricted data. WEAP applications generally include several steps. The study definition sets up the time frame, spatial boundary, system components and configuration of the problem. The WEAP Current Accounts (catchment hydrology without future scenarios) provide a snapshot of actual water demand, pollution loads, resources and supplies for the system. Alternative sets of future assumptions are based on policies, costs, technological development, and other factors that affect demand, pollution, supply and hydrology. Scenarios are constructed consisting of alternative sets of assumptions or policies. Finally, the scenarios are evaluated with regard to water sufficiency, costs and benefits, compatibility with environmental targets, and sensitivity to uncertainty in key variables. The LRB was modelled by several steps starting from creating the entire basin of the catchment and then subdividing the basin into the 114 Quaternary catchments (QC) of the Lepelle River Basin. The Quaternary catchments were automatically created in automatic catchment delineation mode by the help of 3 arc seconds digital elevation model (DEM). Elevation bands were also created automatically because temperature changes with elevation. Land cover categories were also generated. The QCs were then inputted with the 8 km resolution climate data (precipitation, temperature, wind speed and relative humidity) one by one coming to a total of 484 data points. Square kilometre areas for the QCs were adjusted where necessary. The model was calibrated using historical data from the year 1980 to 1996 using streamflow station B7H009 shown Figure 1B of study area. These stations were ones with the second largest area within the LRB and had no missing data within the calibration period. Sensitivity analysis were carried out using some of the model parameters such as the deep conductivity, runoff resistance factor and deep-water capacity. Below is a list of model performance criteria were employed to ascertain the model simulation performance and the results.

A. Descriptive statistics: mean, standard deviation and coefficient of variation (*CV*)
B. Root mean square error (*RMSE*) and mean absolute error (*MAE*)
C. Coefficient of determination (R^2)
D. Nash Sutcliffe coefficient of efficiency (*NSE*)
   a) modified with absolute values of residuals (*NSEj*)
   b) modified by use of relative deviation (E_{rel})
E. Index of agreement (*d*)
   a) modified with absolute values of residuals (*dj*)
   b) modified by use of relative deviation (d_{rel}).

Performance statistics were computed and compared for both simulated and observed streamflow (Tab. 3).

Table 3. Efficiency criteria results for model validation

Assessment criterion	Overall basin
Root mean square error (*RMSE*)	0.107
Mean absolute error (*MAE*)	0.061
Coefficient of determination (*R²*)	**0.706**
Nash–Sutcliffe coefficient of efficiency *NSE*	**0.600**
NSE_j (high flow prediction)	0.995
*NSE*_rel (low flow prediction)	0.723
Index of agreement	0.802
d_j (high flow prediction)	0.607
*d*_rel (low flow prediction)	0.808

Explanation: the values for R^2 and *NSE* are of high importance for validating the model performance.
Source: own elaboration based on model validation results.

DROUGHT ANALYSIS BY DROUGHT INDICES

Reconnaissance drought index (*RDI*)

RDI was developed by TSAKIRIS and VANGELIS [2005]. *RDI* is based on the ratio between cumulative values of precipitation and evapotranspiration (*PET*). The initial value of the *RDI* is obtained by calculating a ratio α_k between the precipitation in a given area and the total potential evapotranspiration for each consecutive period of the *k* months in a year. It is mathematically expressed as follows:

$$\alpha_k = \frac{\sum_{j=1}^{j=k} P_{ij}}{\sum_{j=1}^{j=k} PET_{ij}} \quad i = 1(1)N \text{ and } j = 1(1)k \qquad (1)$$

Where: P_{ij} and PET_{ij} are the precipitation and potential evapotranspiration respectively for the jth and the ith year and *N* is the total number of years. The values of α_k follow satisfactorily both the lognormal and the gamma distributions in a wide range of locations and different time scales, in which they were tested [TIGKAS *et al.* 2013; VANGELIS *et al.* 2013]. Where the lognormal distribution is applied, the following equation can be used for the calculation of RDI_{st}:

$$RDI_{st}^{(i)} = \frac{y^i - \bar{y}}{\hat{\sigma}_y} \qquad (2)$$

Where: y^i is the $(\ln \alpha_k^{(i)})$, $\bar{y}$ is its arithmetic mean and $\hat{\sigma}_y$ is its standard deviation. When the gamma distribution is applied, the RDI_{st} can be calculated by fitting the gamma probability density function (PDF) to the given frequency distribution of αk [TIGKAS *et al.* 2013; VANGELIS *et al.* 2013]. For short reference periods (e.g. monthly or 3-months) which may include zero values for the cumulative precipitation of the period, the RDI_{st} can be calculated based on a composite cumulative distribution function which includes:
– the probability of zero precipitation,
– the gamma cumulative probability.

RDI is calculated for a hydrological year in 3-, 6-, 9- and 12-month reference periods. This shows the different nature of *RDI* in comparison to other drought indices, since *RDI* is calculated for predetermined reference periods and not as a "rolling" index of constant duration. So, *RDI* in this study was used to calculate meteorological drought index. Table 4 shows *RDI* based drought classification.

Table 4. Reconnaissance drought index (*RDI*) based drought classification

State	Description	*RDI* criterion
1	mild drought	(–0.5) – (–1.0)
2	moderate drought	(–1.0) – (–1.5)
3	severe drought	(–1.5) – (–2.0)
4	extreme drought	< –2.0 and below

Source: TIGKAS *et al.* [2013].

Streamflow drought index (*SDI*)

SDI provides a good estimate of hydrological drought in any given area. The *SDI* focuses directly on the drought because of abnormally low flow conditions. So given a time series of monthly streamflow volumes Q_{ij}, in which *i* denotes the hydrological year and *j* the month within that hydrological year (*j* = 1 for October and j = 12 for September), V_{ik} can be obtained based on the equation:

$$V_{ik} = \sum_{j=1}^{3k} Q_{ij} \quad i = 1, 2 \ldots, j = 1, 2 \ldots, 12 \quad k = 1, 2, 3, 4.. \quad (3)$$

Where: V_{ik} is the cumulative streamflow volume for the ith hydrological year and the kth reference period, *k* = 1 for October–December, *k* = 2 for October–March, *k* = 3 for October–June, and *k* = 4 for October–September. Based on the cumulative streamflow volumes V_{ik} the streamflow drought index (*SDI*) is defined for each reference period *k* of the ith hydrological year as follows:

$$SDI_{ik} = \frac{V_{ik} - \bar{V}_k}{S_k} \quad i = 1, 2, .., k = 1, 2, 3, 4 \qquad (4)$$

in which $\bar{V}_k$ and S_k are respectively the mean and the standard deviation of cumulative streamflow volumes of the reference period *k* as these are estimated over a long period of time. In this definition the truncation level is set to $\bar{V}_k$ although other values based on rational criteria could be also used. Table 5 shows the *SDI* drought classification.

Table 5. Streamflow drought index (*SDI*) based drought classification

State	Description	*SDI* criterion
0	non-drought	≥ 0.0
1	mild drought	(–1.0)–(0.0)
2	moderate drought	(–1.5)–(–1.0)
3	severe drought	(–2.0)–(–1.5)
4	extreme drought	< –2.0 and below

Source: TIGKAS *et al.* [2013].

Probability distribution functions (PDFs) selection

Various distribution functions exist in hydrological modelling. In order to minimise computation, the SigmaXL model was used to determine the PDF with best fit where possible. SigmaXL uses the Anderson Darling *p*-value (AD *p*-value) as the criteria to determine best fit. All distributions and transformations are considered and the model with the highest AD *p*-value is initially selected (denoted as adpvalmax). A search is then carried out for models that are close, having an AD *p*-value greater than adpvalmax 0.1 (with an added criterion that AD *p*-value be >0.2), but having fewer parameters than the initial best fit

model. If a simpler model is identified, then this is selected as the best fit [SigmaXL Inc. 2019].

RESULTS AND DISCUSSIONS

DROUGHT DISTRIBUTION

The best fit distributions where used for the PDFs but are not shown here together with their transformations to normal. This PDFs were computed using both the maximum likelihood parameter of estimation the Log-likelihood estimation parameter where necessary using [SigmaXL 2019]. This is an advantage over most distribution methods. The Johnson distribution was found to be the most suited distributions for majority of the Quaternary catchments (QCs). The Johnson distribution is categorised into a family of probability distributions first investigated by N.L. Johnson in 1949. These include the SU, SB and SL families where S stands for the specification limits of U – unbounded distribution, B – bounded distribution, and L – log-normal distribution. For this region, the Johnson's SB family (JSB) dominated. The capability of JSB in estimating the integral parameters, especially rainfall rate (R) and reflectivity (Z), results very close to that of gamma distribution. In particular, for light precipitation, JSB is superior to with fractional standard error (FSE) of 11% with respect to values ranging between 25% and 37% for gamma [TOKAY et al. 2016]. Also, recent studies have shown that the Gamma distribution is not a one size fits all for all locations and data type [AYODELE, OGUNJUYIGBE 2015; GYAMFI et al. 2019]. But it is still a good PDF for most regions and data types.

The use of different statistical distributions in describing the probabilistic nature of streamflow suggests the inhomogeneity of records arising mainly from dissimilarities in physical characteristics, climatic tendencies, hydrological regimes, and hierarchy. Therefore, the use of different statistical distributions that best fit the local context is admonished. This agrees with studies by GYAMFI et al. [2019]. An ideal statistical distribution irrespective of the geographic location must be one that is flexible enough to fit the full range of observations under consideration. For this reason, all the drought indices where distributed with the Gamma distribution since it was the closest available distribution to the Johnson's for the computations in the DrinC software described by [VANGELIS et al. 2013].

METEOROLOGICAL AND HYDROLOGICAL DROUGHT

In Figures 2 and 3, on the left-hand side and the right-hand side are charts showing the meteorological and hydrological drought indices using reconnaissance drought index (*RDI*) and streamflow drought index (*SDI*) respectively. The magnitudes of the drought can be determined from Figures 2 and 3 by classifying the drought using Tables 3 and 4 respectively. For RCP8.5 it can be seen from Figure 2, that years where the indices show a dip below zero indicate dryer years ranging from mild to severe and extreme cases of meteorological drought. A cursory view of the chart B71H for both *SDI* and *RDI* reveals for in-

stance that the lower Lepelle River Basin will experience a mild meteorological drought between 2022 and 2024. A predicted hydrological drought (*SDI*) appears to lag the meteorological drought by 1.5 years and is noticeable from 2023–2025. Also, an extreme meteorological drought is forecast between 2046 and 2048 while for the associated hydrological drought is forecast between 2047 and 2048 under RCP8.5. This observation is expected since hydrological drought only becomes visible after meteorological drought has occurred. Again, a consistent increase in hydrological drought magnitude is observed for catchment B42A and B71H under RCP4.5. It is pertinent to highlight that as the 22nd century is approached, drought and flood events begin to occur for longer durations and at a higher frequency. Also, because the volume of water in the Earth is constant (1 386 billion km^3) [BLEAMASTER, CROWN 2010], it then is a truism that higher drought frequencies invariably means higher flood frequencies. This is because energy can neither be created nor destroyed in order to maintain the constant volume of water. Also, the impact of climate change is accentuated when one compares the frequency of drought for the future and historically (Figs. 2, 3). There is a much higher frequency of droughts and floods as we approach the 22nd century than it is now and in the past. Of course, this observation assumes nothing is done and we head into the 22nd century with increasing concentrations of carbon dioxide emissions and increasing population growth trends.

MANN–KENDALL TREND TEST

The seasonal and annual non-parametric test for trends in drought patterns was carried out using Mann–Kendall test and for the 6 cases 4 showed that at $\alpha = 0.001$ or at 0.1% significance level the null hypothesis of no trend could be rejected. However, the remaining two cases which were for the Upper Lepelle River (B11B) for both RCPs, the annual test shows a trend at a significance level greater than 10% as observed in Table 6 in the rows with + sign and the blank rows depicting these trends.

Although droughts are observed, complimentary severe wet episodes are also predicted which appear to be more frequent than observed during the historical data. Thus, the total annual flow does not appear to be affected significantly but will differ in timing and seasonality for most of the LRB under RCP4.5; except for the middle and lower reaches.

CORRELATION BETWEEN *RDI* AND *SDI* DROUGHT INDICES

Lastly, Spearman and Pearson correlation test and multiple regression (method of least squares) analyses (R^2) were performed to determine how the meteorological and hydrological drought indices were related. In Table 7, the correlation indices were compared and the ones having Spearman indicate that Spearman showed stronger positive correlation than Pearson except in row 3 of column 2 where Pearson was the stronger of the 2.
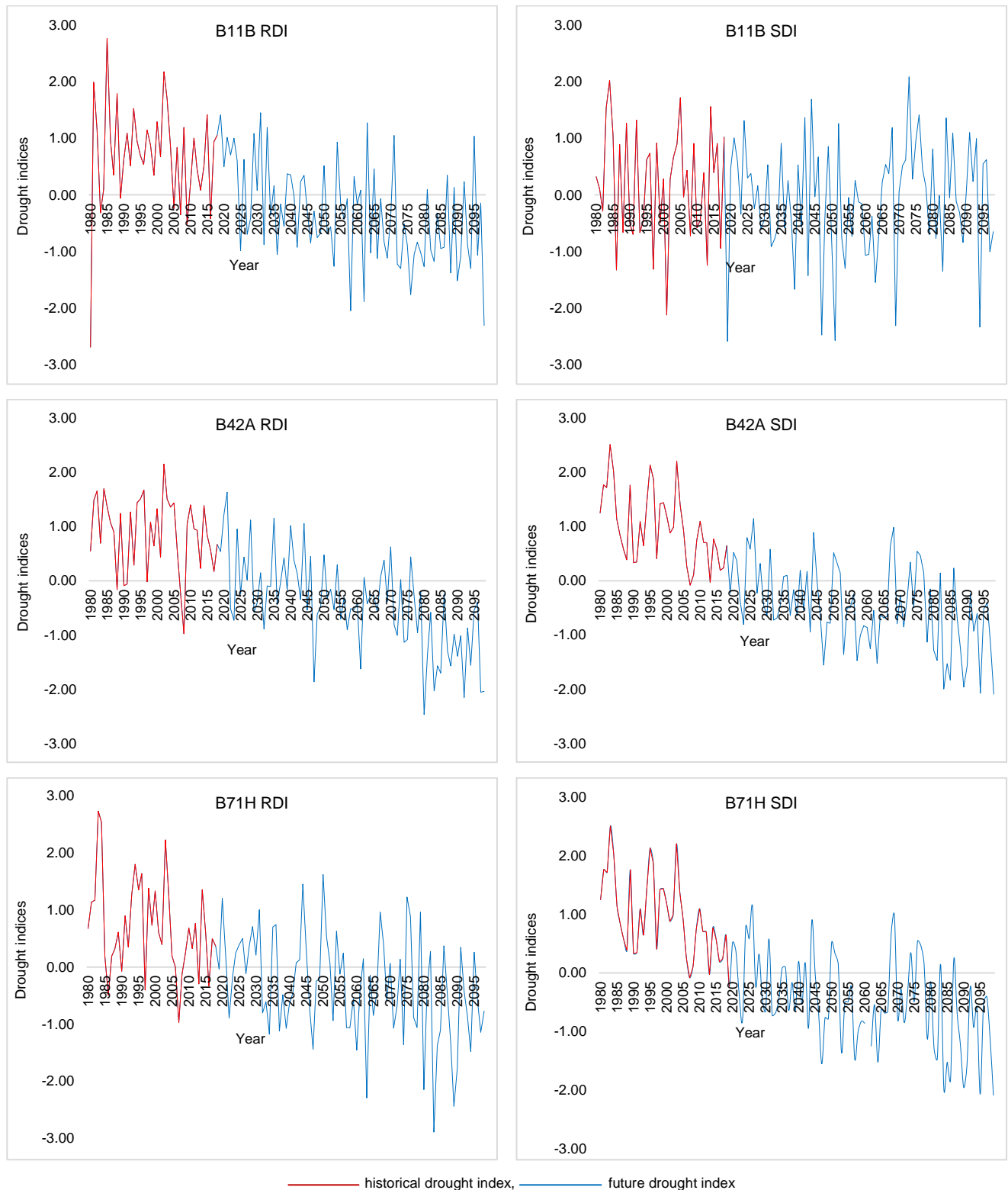
Fig. 2. Reconnaissance drought index (*RDI*) and streamflow drought index (*SDI*) forced by representative concentration pathway RCP8.5 in Quaternary catchments (B11B, B42A and B71H); RCP8.5 = the highest or worst case global emission scenario which could result in an increase of temperature to about 3.2–5.4°C as we heard to the 21st century; source: own study
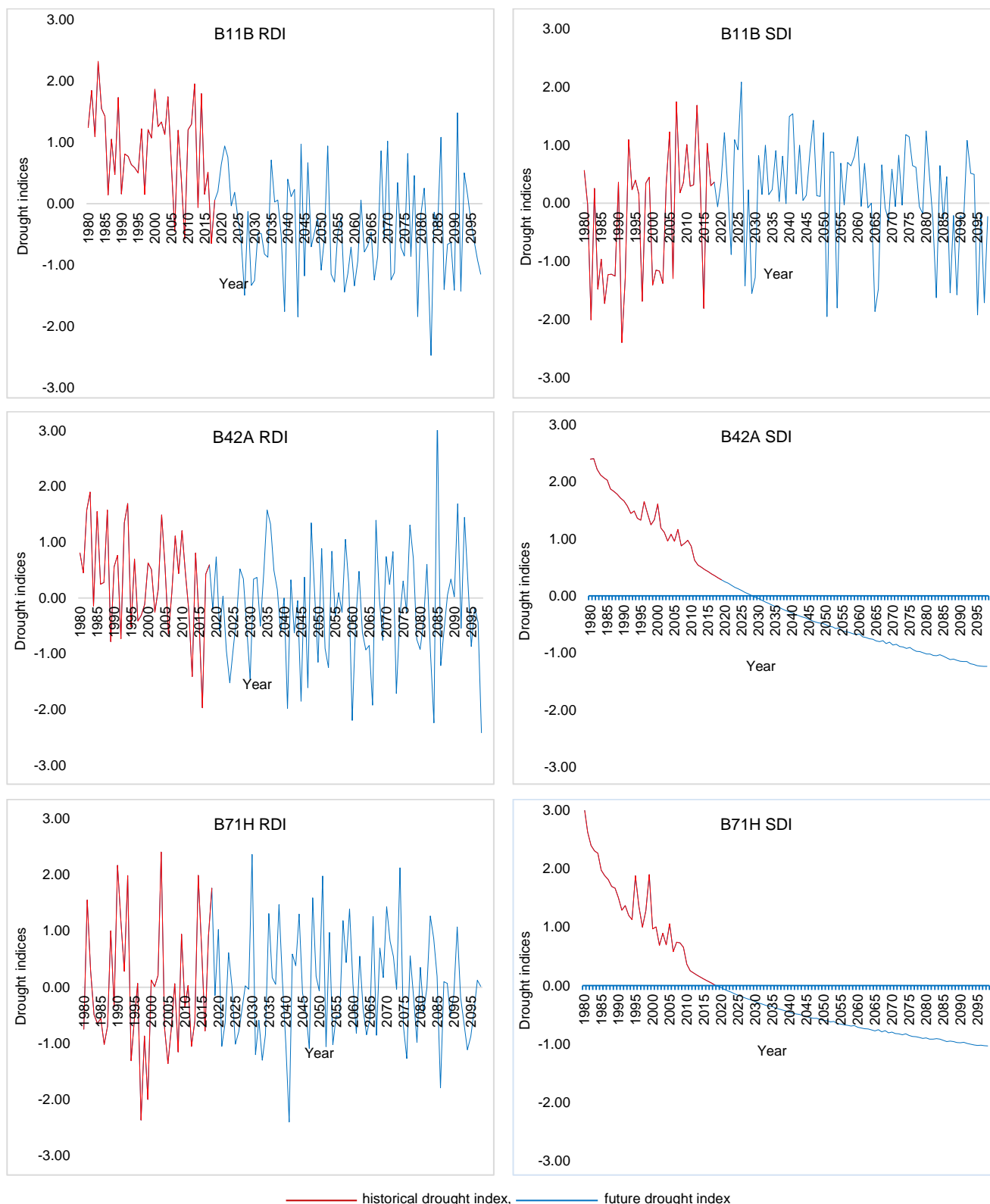
Fig. 3. Reconnaissance drought index (*RDI*) and streamflow drought index (*SDI*) forced by representative concentration pathway RCP4.5 in Quaternary catchment (B11B, B42A and B71H); RCP4.5 = scenario of long-term, global emissions of greenhouse gases, short-lived species, and land-use-land-cover which stabilizes radiative forcing at 4.5 $W \cdot m^{-2}$ in the year 2100 without ever exceeding that value; source: own study

Table 6. Mann–Kendall annual and seasonal trend test results for the Upper Lepelle River (B11B) for representative concentration pathways RCP4.5 and RCP8.5 (first year 1980, last year 2098)

Time series	Test Z (RCP4.5)	Test Z (RCP8.5)	Significance (RCP4.5)	Significance (RCP8.5)
October	–1.35	–3.98		***
November	–1.34	3.01		**
December	–2.72	2.45	**	*
January	0.49	1.31		
February	–3.44	0.24	***	
March	–1.96	–2.30	+	*
April	–4.10	–2.13	***	*
May	–3.89	–0.72	***	
June	–2.45	–0.76	*	
July	–3.90	–0.69	***	
August	–1.78	–1.58	+	
September	–2.31	–3.05	*	**
Annual	0	–0.92		
Winter	–2.28	–0.80	*	
Spring	–0.92	–4.92		***
Summer	–2.08	3.50	*	***
Autumn	–4.61	–2.05	***	*

Explanations: RCP4.5 = as in Fig. 3; RCP8.5 = as in Fig. 2; *** if trend at $\alpha = 0.001$ level of significance, ** if trend at $\alpha = 0.01$ level of significance, * if trend at $\alpha = 0.05$ level of significance, + if trend at $\alpha = 0.1$ level of significance. If the cell is blank, the significance level is greater than 0.1 [SALMI *et al.* 2002].
Source: own study.

Table 7. Correlation matrix for reconnaissance drought index (*RDI*) and streamflow drought index (*SDI*) forced by representative concentration pathways RCP8.5 and RCP4.5

Quaternary catchment	RCP	Correlation matrix ($p < 0.05$)	R^2	Adjusted R^2
B11B		0.3629 – Spearman	0.0037	0.0
B42A	8.5	0.8462 – Spearman	0.6949	0.6923
B71H		0.8259 – Spearman	0.7040	0.7015
B11B		0.0034 – Spearman	0.0	0.0
B42A	4.5	0.276 – Pearson	0.0762	0.0683
B71H		0.045 – Spearman	0.0027	0.0

Explanations: Quaternary catchments as in Figure 1; RCP8.5, RCP4.5 as in the Tables 5 and 6 respectively; R^2 = determination coefficient.
Source: own study.

The two QCs drought indices under RCP8.5 exhibit a strong positive correlation while a weak to no correlation is observed for the remaining catchments. A possible explanation for this could be that, in the future, different water management schemes and decisions are likely to be implemented for the various catchments of the LRB.

DISCUSSION

Looking at chart 11B between 2057 and 2059 under RCP8.5 a mild meteorological drought is observed. While this is not severe it is worth noting that it is a departure from the normal judging from history between 1980–2019 for the upper Lepelle River Basin. A striking contrast is however observed from 2058 when a severe drought occurs. While this may not be an urgent concern given the lead time available to act, measures must be put in place given the duration of this droughts which impact may be felt for five consecutive years between 2058 and 2063. On

the other hand, hydrological drought as observed by *SDI* drought indices show more severe droughts along through to the end of the 21st century. These slight discrepancies between meteorological and hydrological drought indices begs the question for the differences. These differences could be as a result of unsupervised indiscriminate abstraction of water from streams due increasing population and unsustainable water use. Note that RCP8.5 scenario has been used to model this hydrology in this case which supports more urbanisation and industrialisation as seen in Table 8. The increase in population can be attributed to the rapid urbanisation in the upper LRB due to income opportunities from mining activities seeing that the LRB is rich in coal deposits and accounts for more than 50% of South Africa's coal-fired electricity plants [DE LANGE *et al.* 2005]. Another source of income are the tourist attractions such as the Kruger National Park and the Blyde River Canyon [DWS 2018]. The middle and lower LRB represented in Figure 2 by B42A and B71H respectively however, shows similar meteorological and hydrological drought pattern. Again, one can see that because the population of these two areas are fairly constant, hence perhaps water abstraction is fairly stable.

Table 8. Summary of scenarios adopted for the future the Lepelle River Basin (LRB) hydrology model

Scenario	Climate variable	Land-use	WC/WDM	Population growth (%)	Case
1	RCP8.5	pro-industrialisation	high growth (25%)	1.55	worst
2	RCP4.5	pro-agriculture	moderate growth (15%)	1.20	medium

Explanations: RCP8.5 and RCP4.5 as in the Tables 5 and 6 respectively. WC = water conservation, WDM = water demand management.
Source: own study.

Now in Figure 3 modelled by RCP4.5 the Upper LRB appears to be very similar given that abstractions will stabilize over time. A rather fascinating observation is seen in the middle (B42A) and lower LRB (B71H) under RCP4.5 for hydrological drought indicated by the *SDI*. A possible reason for the mild but constant hydrological drought could be as a result of future water abstraction for agricultural irrigation purposes given that it is pro-agriculture as shown in Table 8.

So, while the future looks disturbing for some of the catchments of the LRB namely all troughs below 0 indicating droughts and are seen to be more persistent as we approach the end of the 21st century. These can be observed in B42A RDI, B42A SDI, B71H RDI, B42A SDI for RCP8.5 and also observed in B11B RDI, B42A SDI and B71H SDI for RCP4.5, it is relieving to note that with timely interventions water availability can still be guaranteed. These interventions could range from building more dams to harvest flood waters from the extreme wet periods, curbing illegal water abstractions, water-shedding, reducing carbon emissions by using more environmentally friendly technologies etc.

The 8 km resolution data was very much useful in identifying the unique and localised hydrological variations into the future of the LRB.

CONCLUSIONS

The drought situation and water availability of the Lepelle River Basin (LRB) are modelled for the period of 2020–2099. Firstly, the probability distribution functions for the climate variables of the LRB, particularly rainfall and streamflow. Secondly, using two comprehensive drought indices for three representative catchments B11B, B42A and B71H of the 114-Quaternary catchment of the LRB under two representative concentration pathways (RCP) forcings, the future drought characteristics were explored. Lastly, Mann–Kendall trend tests were conducted coupled with correlation and multiple regression analysis for the drought indices at a significance level of $p < 0.05$.

1. The Johnson's specification limit of bounded family of probability density function (PDF) was the best fit for the models and the Gamma PDF was equally acceptable.

2. The reconnaissance drought index (*RDI*) and streamflow drought index (*SDI*) showed varying characteristics of drought for different areas of the LRB.

3. Drought indices revealed a varying degree of magnitude and periodicity for the different catchments under the two RCPs.

4. A mild meteorological drought is predicted for the lower LRB under RCP8.5 between 2022 and 2024.

5. It is worth noting that a mild but increasing trend of drought is predicted as the 22nd century is approached for the middle and lower LRB under RCP4.5.

6. Modelling indicates that droughts and floods will occur more frequently and for longer periods.

7. In absolute terms, total amount of annual rainfall and streamflow seems to mirror current levels, but the timing and the variability of these variable are predicted to be impacted by climate change and hence could be problematic for water use planning and agricultural purposes.

The modelling indicates that the absolute total amounts of annual rainfall and streamflow will match current levels, but the timing and variability of these variables will be affected by climate change and hence could be problematic for planning and agricultural purposes. Thus, the simulations suggest that mitigations measures against drought and flooding will have to be implemented in the LRB in the very near future. The closest mild-moderate drought period is forecast for 2022–2024 and is seen in the B71H catchment under RCP4.5 which leaves less margin for preparation and for the development and implementation of mitigation measures in a predominantly rural area such as the Lepelle River Basin.

REFERENCES

AHNERT M., BLUMENSAAT F., LANGERGRABER G., ALEX J., WOERNER D. 2007. Goodness-of-fit measures for numerical modelling in urban water management – A summary to support practical applications. 10th IWA Specialised Conference on Design, Operation and Economics of Large Wastewater Treatment Plants. 9–13.09.2007 Vienna p. 69–72.

AYODELE T.R., OGUNJUYIGBE A.S.O. 2015. Prediction of monthly average global solar radiation based on statistical distribution of clearness index. Energy. Vol. 90 p. 1733–1742. DOI 10.1016/j.energy.2015.06.137.

BENTSEN M., BETHKE I., DEBERNARD J.B., IVERSEN T., KIRKEVÅG A., SELAND Ø., … KRISTJÁNSSON J.E. 2013. The Norwegian Earth System Model, NorESM1-M. Part 1: Description and basic evaluation of the physical climate. Geoscientific Model Development. Vol. 6. Iss. 3 p. 687–720.

BLEAMASTER L.F., CROWN D.A. 2010. Eastern Hellas Planitia Region of Mars Pamphlet to accompany Scientific Investigations Map 3096. U.S. Geological Survey Geologic Investigations, 3096, 80225.

BORDERIES M., CAUMONT O., DELANOË J., DUCROCQ V., FOURRIÉ N. 2019. Assimilation of wind data from airborne Doppler cloud-profiling radar in a kilometre-scale NWP system. Natural Hazards and Earth System Sciences. Vol. 19. Iss. 4 p. 821–835. DOI 10.5194/nhess-19-821-2019.

COLLINS W.D., BITZ C.M., BLACKMON M.L., BONAN G.B., BRETHERTON CH.S., CARTON J.A. … SMITH R.D. 2006. The Community Climate System Model Version 3 (CCSM3). Journal of Climate. Vol. 19(11) p. 2122–2143. DOI 10.1175/JCLI3761.1.

CONDIE R., LEE K. A. 1982. Flood frequency analysis with historic information. Journal of Hydrology. Vol. 58. Iss. 1–2 p. 47–61.

DALRYMPLE T. 1960. Flood-frequency analyses. Manual of hydrology. Part 3. Flood-flow techniques. USGPO. Geological Survey Water – Supply Paper. No. 1543-A. Washington. USGPO pp. 80.

DE LANGE M., MERREY D.J., LEVITE H., SVENDSEN M. 2005. Water resources planning and management in the Olifants Basin of South Africa : Past, present and future. In: Irrigation and river basin management: Options for governance and institutions. Ed. M. Svendsen. CABI p. 145–168.

DWS 2018. Integrated water quality management plan for the Olifants River System. Report No. 12. Monitoring Programme.

ENGELBRECHT F.A., LANDMAN W.A., ENGELBRECHT C.J., LANDMAN S., BOPAPE M.M., ROUX B., … THATCHER M. 2011. Multi-scale climate modelling over Southern Africa using a variable-resolution global model. Water SA. Vol. 37(5) p. 647–658.

GIORGETTA M.A., JUNGCLAUS J., REICK CH.H.; LEGUTKE S., BADER J., BÖTTINGER M. … STEVENS B. 2013. Climate and carbon cycle changes from 1850 to 2100 in MPI-ESM simulations for the Coupled Model Intercomparison Project phase 5. Journal of Advances in Modeling Earth Systems. Vol. 5(3) p. 572–597. DOI 10.1002/jame.20038.

GONZÁLEZ J., VALDÉS J.B. 2010. The mean frequency of recurrence of in-time-multidimensional events for drought analyses. Natural Hazards and Earth System Science. Vol. 4(1) p. 17–28. DOI 10.5194/nhess-4-17-2004.

GYAMFI CH., AMANING-ADJEI K., ANORNU G.K., NDAMBUKI J. M., ODAI S.N. 2019. Evolutional characteristics of hydrometeorological drought studied using standardized indices and wavelet analysis. Modeling Earth Systems and Environment. Vol. 5 p. 455–469.

KUBHEKA A. 2019. Are tornadoes becoming more frequent in KZN ? [online]. IOL. Nov 25, 2019. [Access 25.11.2019]. Available at: https://www.iol.co.za/dailynews/news/kwazulu-natal/are-tornadoes-becoming-more-frequent-in-kzn-37934763

LEE J.-H., KWON H.-H., JANG H.-W., KIM T.-W. 2016. Future changes in drought characteristics under extreme climate change over South Korea. Advances in Meteorology. Vol. 2016. Art. ID 9164265 p. 1–19.

LEE J.-H., SEO J.-W., KIM CH.-J. 2012. Analysis on trends, periodicities and frequencies of Korean drought using drought indices. Journal of Korea Water Resources Association. Vol. 45(1) p. 75–89. DOI 10.3741/JKWRA.2012.45.1.75.

LIN S.-J., CHAO W.C., SUD Y.C., WALKER G.K. 1994. A class of the van Leer-type transport schemes and its application to the moisture transport in a general circulation model. Monthly Weather Review. Vol. 122(7) p. 1575–1593.

MAGHSOOD F.F., MORADI H., BAVANI A.R.M, PANAHI M., BERNDTSSON R., HASHEMI H. 2019. Climate change impact on flood frequency and source area in northern Iran under CMIP5 scenarios. Water. Vol. 11(2). DOI 10.3390/w11020273.

MAURER E.P. 2007. Uncertainty in hydrologic impacts of climate change in the Sierra Nevada, California, under two emissions scenarios. Climatic Change. Vol. 82(3–4) p. 309–325.

ORSINI-ZEGADA L., ESCALANTE-SANDOVAL C. 2016. Flood frequency analysis using synthetic samples. Atmosfera. Vol. 29(4) p. 299–309. DOI 10.20937/ATM.2016.29.04.02.

PARKS R., MCLAREN M., TOUMI R., RIVETT U. 2019. Experiences and lessons in managing water from Cape Town, Grantham Institute Briefing Papers. No. 29 p. 1–20.

POLLARD S., RETIEF H., NETHENGWE M. 2018. Workshop Report Lower Olifants River Network LORiN Inaugural network workshop for the sustainability of water resources in the lower Olifants River. Limpopo. AWARD pp. 40.

PURI K. 2005. The Australian Community Climate and Earth System Simulator [online]. ACCESS. [Access 10.07.2019]. Available at: https://pdfs.semanticscholar.org/827b/ecfec27ed60d3e640bdd9959bb91df138709.pdf

RIAHI K.M RAO S., KREY V., CHO CH,, CHIRKOV V., FISCHER G., … RAFAJ P. 2011. RCP 8.5 – A scenario of comparatively high greenhouse gas emissions. Climatic Change. Vol. 109(1). Art. No. 33.

SALMI T., MAATTA A., RUOHO-AIROLA T., AMNELL T. 2002. Detecting trends of annual values of atmospheric pollutants by the Mann-Kendall Test and Sen's slope estimates – The Excel template application Makesens. Ilmanlaadun julkaisuja Publikationer om luftkvalitet Publications on air quality. No. 31. Ilmatieteen laitos. Helsinki. Meteorologiska Institutet, Finnish Meteorological Institute pp. 35.

SCHMIDLI J., GOODESS C.M., FREI C., HAYLOCK M.R., HUNDECHA Y., RIBALAYGUA J. 2007. Statistical and dynamical downscaling of precipitation: An evaluation and comparison of scenarios for the European Alps. Journal of Geophysical Research Atmospheres. No. 112(4) p. 1–20. DOI 10.1029/2005JD007026.

SEMENOV M.A., BARROW E.M. 1997. Use of a stochastic weather generator in the development of climate change scenarios. Climatic Change. Vol. 35 p. 397–414.

SigmaXL Inc. 2019. SigmaXL Ver. 8.1. Workbook pp. 563.

SMID M., COSTA A.C. 2018. Climate projections and downscaling techniques: A discussion for impact studies in urban systems. International Journal of Urban Sciences. Vol. 22(3) p. 277–307.

SPINONI J., NAUMANN G., CARRAO H., BARBOSA P., VOGT J. 2014. World drought frequency, duration, and severity for 1951–2010. International Journal of Climatology. Vol. 34(8) p. 2792–2804. DOI 10.1002/joc.3875.

THATCHER M., MCGREGOR J., DIX M., KATZFEY J. 2015. A new approach for coupled regional climate modeling using more than 10,000 cores. IFIP Advances in Information and Communication Technology. Vol. 448 p. 599–607.

THOMSON A.M., CALVIN K.V., SMITH S.J., KYLE G.P., VOLKE, A., PATEL P., … EDMONDS J.A. 2011. RCP4.5: A pathway for stabilization of radiative forcing by 2100. Climatic Change. Vol. 109(1). Art. No. 77.

TIGKAS D., VANGELIS H., TSAKIRIS G. 2013. The drought indices calculator (DrinC). In: Proceedings of 8th International Conference of EWRA Water Resources Management in an Interdisciplinary and Changing Context. Eds. R. Maia, A. Guerreiro de Brito, A. Seca Teixeira, J. Tentúgal Valente, J.P. Pêgo. Porto, Portugal. 26–29.06.2013 p. 1333–1342.

TOKAY A., D'ADDERIO L.-P., WOLFF D.B., PETERSEN W.A. 2016. A field study of pixel-scale variability of raindrop size distribution in the Mid-Atlantic Region. Journal of Hydrometeorology. Vol. 17(6) p. 1855–1868. DOI 10.1175/JHM-D-15-0159.1.

TSAKIRIS G., VANGELIS H. 2005. Establishing a drought index incorporating evapotranspiration. European Water. Vol. 9(10) p. 3–11.

TURNER B.L., SABLOFF J.A. 2012. Classic period collapse of the Central Maya Lowlands: Insights about human-environment relationships for sustainability. In: Proceedings of the National Academy of Sciences of the United States of America. Vol. 109(35) p. 13908–13914. DOI 10.1073/pnas.1210106109.

VANGELIS H., TIGKAS D., TSAKIRIS G. 2013. The effect of PET method on reconnaissance drought index (RDI) calculation. Journal of Arid Environments. Vol. 88 p. 130–140. DOI 10.1016/j.jaridenv.2012.07.020.

WATKINS K. 2007. Human development report 2007/2008: fighting climate change: Human solidarity in a divided world. New York. UNDP. ISBN 978-0-230-54704-9 pp. 384.

WAYNE G.P. 2013. The Beginner's guide to Representative Concentration Pathways (RCPs). Ver. 1.0. SkepticalScience pp. 24.

WISE M., CALVIN K., THOMSON A., CLARKE L., BOND-LAMBERTY B., SANDS R., … EDMONDS J. 2009. Implications of limiting CO_2 concentrations for land use and energy. Science. Vol. 324(5931) p. 1183–1186. DOI 10.1126/science.1168475.

YOO J., KWON H.H., KIM T.-W., AHN J.-H. 2012. Drought frequency analysis using cluster analysis and bivariate probability distribution. Journal of Hydrology. Vol. 420–421 p. 102–111. DOI 10.1016/j.jhydrol.2011.11.046.

ZHU J., SUN G., LI W., ZHANG Y., MIAO G., NOORMETS A., … WANG X. 2017. Modeling the potential impacts of climate change on the water table level of selected forested wetlands in the southeastern United States. Hydrology and Earth System Sciences. Vol. 21(12) p. 6289–6305. DOI 10.5194/hess-21-6289-201.